Geochemical Perspectives Letters

Silver isotope fractionation by chemical diffusion in granitic melt

S. Li, L. Zhang, Y. Fang, H. Ni, F. Huang

Supplementary Information

The Supplementary Information includes:

- Starting Glasses
- Experimental Methods
- Analytical Methods
- Tables S-1 to S-3
- Figures S-1 to S-4

Starting Glasses

Diffusion couple experiments were performed with two anhydrous glasses of the same major element but different Ag contents. The target granitic composition used in this study has previously been used to assess the diffusivities of Cu, Mo, W, and Ag (Ni *et al.*, 2018; Zhang *et al.*, 2018, 2021). The target composition was 70.68 % SiO_2, 15.64 % Al_2O_3, 0.57 % MgO, 1.77 % FeO_t, 0.23 % TiO_2, 4.69 % K_2O, 3.95 % Na_2O and 1.7 % CaO. The anhydrous granitic glass was synthesised by melting a mixture of oxides (17.81 g SiO_2, 3.94 g Al_2O_3, 0.14 g MgO, 0.50 g Fe_2O_3 and 0.06 g TiO_2) and carbonates (1.73 g K_2CO_3, 1.70 g Na_2CO_3 and 0.76 g $CaCO_3$) at 1000 °C in a muffle furnace for 10 h to decarbonate, then at 1550 °C for 4 h twice. The glass powder was divided into two portions. One portion was doped with approximately 400 µg/g Ag_2O, and the other with around 2000 µg/g Ag_2O. Subsequently, both of them were remelted in a Pt crucible at 1550 °C for 4 h to obtain low-Ag and high-Ag glasses, respectively. To ensure a homogeneous distribution of Ag, the doped glasses were crushed and remelted again at 1550 °C for an additional 4 h.

The synthesized glasses were then examined under an optical microscope. It was observed that they were crystal-free and homogeneous in colour, and all the glasses contained a small amount of air bubbles, less than 1 % by volume. The average compositions of the synthesised glasses are given in Table S-1. The Ag content of the low-Ag glasses was determined to be 25–36 µg/g and that of the high-Ag glasses to be 190–310 µg/g. Ag content variation in the glass used for the two experiments was <5 %, which can be considered homogenous.

Experimental Methods

The diffusion experiments were performed in a ¾" end-loaded piston-cylinder apparatus. The experimental procedure was started with the drilling of two types of glass cylinders (one fabricated from high-Ag glass and the other from low-Ag glass), each with a diameter of 2.5 mm and a height between 1.8 and 2.4 mm. The glass cylinders were doubly polished, then assembled within a graphite capsule with an outer diameter of 4.6 mm. Glass with a slightly lower density (low-Ag glass) was placed on top of the high-Ag glass. Then the graphite capsule was welded shut in a 5 mm outer diameter, 0.2 mm wall thickness Pt capsule. Subsequently, the Pt capsule was fit into a crushable MgO, then placed inside a graphite heater, and then into a borosilicate glass, with the outermost being talc (Fig. S-1). A type-S thermocouple was employed to monitor the temperature, with the data being recorded concurrently by a computer program.

Subsequent to pressurization to the target pressure (1 GPa) in the piston cylinder apparatus, the temperature was raised to 473 K. After 2 h, the two experiments were rapidly heated to 1273 K and 1473 K with a rate of approximately 70 K/s. The temperature and pressure variations were maintained within 10 K and 5 % of the mean value, respectively. Following a duration of 57.69 min and 9.49 min, the power was shut off, resulting in rapid quenching processes (~100 K/s).

Analytical Methods

All analyses were conducted at the State Key Laboratory of Lithospheric and Environmental Coevolution, USTC.

The major element compositions of the granitic glasses, both prior to and following the diffusion experiments, were analysed using a JEOL JXA-8530F Plus electron microprobe. The analysis was conducted using a defocused beam with settings of 15 kV, 10 nA, and a spot size of 10 μm. Each spot analysis was consisted of a duration of 10 s data acquisition and 5 s background acquisition.

Ag concentration of granitic glasses, both prior to and following the diffusion experiments, were measured at USTC, using a Coherent ArF excimer UV 193 nm wavelength Laser ablation system (GeoLas pro) coupled with PerkinElmer ELAN DRC II or Agilent 7700e quadrupole ICP-MS. Spot analyses were conducted using a beam diameter of 30 μm and a repetition rate of 8 Hz. Each spot analysis involved 40 s of data acquisition after 20 seconds of background acquisition. Technical details of the measurement procedures can be found in Hou *et al.* (2020).

Chemical digestion and purification processes for Ag isotope analysis were performed in an ISO Class 6 clean room. Since the content of each element in the diffusion experimental samples was known, using a cation resin AG50 W-X8 was enough to separate Ag. The resin was filled in Savillex microcolumns after cleaning. During the analysis, each sample was analysed a minimum of three times in parallel, a bracketing standard with NIST SRM978a serving as a reference material to correct for instrumental mass bias. To monitor instrumental stability, after analysing four samples each time, AAS-Ag solution was measured. More details can be found in Fang *et al.* (2024).

Supplementary Tables

Table S-1 Chemical compositions of the synthesized granitic glasses analysed by EMPA (in wt. %).

oxide	SiO_2	TiO_2	Al_2O_3	FeO	MgO	CaO	Na_2O	K_2O	Total
wt. %	72.56	0.23	15.11	1.76	0.55	1.62	3.75	4.41	99.98

Table S-2 Conditions and results of Ag diffusion experiments.

Experiment	P (GPa)	T (K)	t (s)	D(m^2/s)	β
LSTAg2	1	1473	569.4	1.26E-10	0.274 ± 0.016
LSTAg3	1	1273	3461.4	3.30E-11	0.317 ± 0.036

Table S-3 Ag isotope composition measured on diffusion couples.

Experiment	Distance (µm)	δ^{109}Ag (‰)	2 s.d. (‰)
LSTAg2	-1750	4.74	0.03
	-1350	4.28	0.08
	-950	2.95	0.09
	-450	2.41	0.09
	50	4.43	0.22
	550	4.69	0.01
	950	4.37	0.01
	1350	4.28	0.07
LSTAg3	-1700	4.45	0.05
	-1150	3.64	0.01
	-700	2.10	0.05
	-250	2.50	0.05
	200	3.61	0.08
	650	4.90	0.04
	1100	4.85	0.09
	1550	4.31	0.02

Supplementary Figures

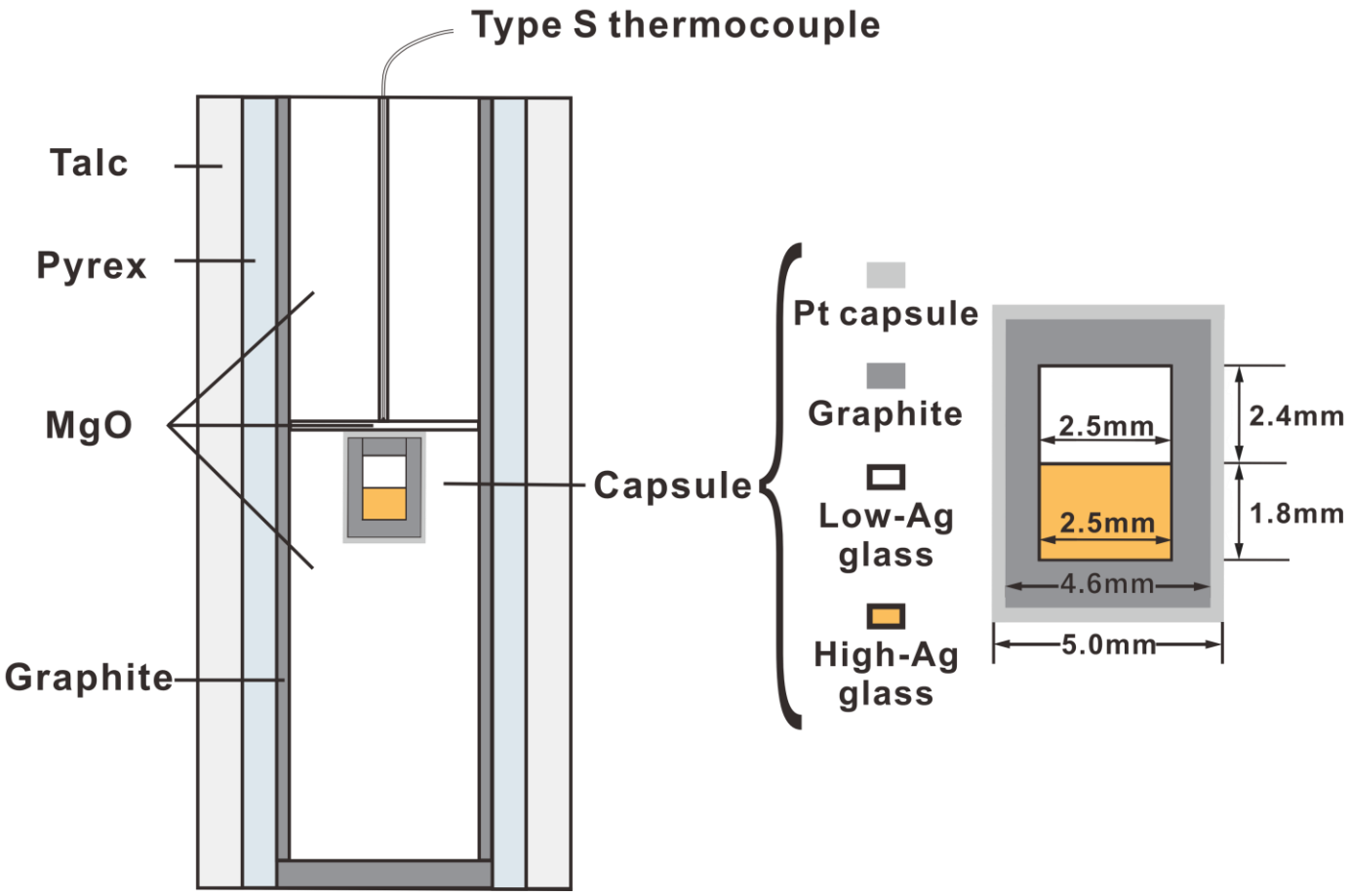

Figure S-1 Illustration of the ¾" piston-cylinder assembly to investigate Ag diffusion and fractionation in granitic melt.

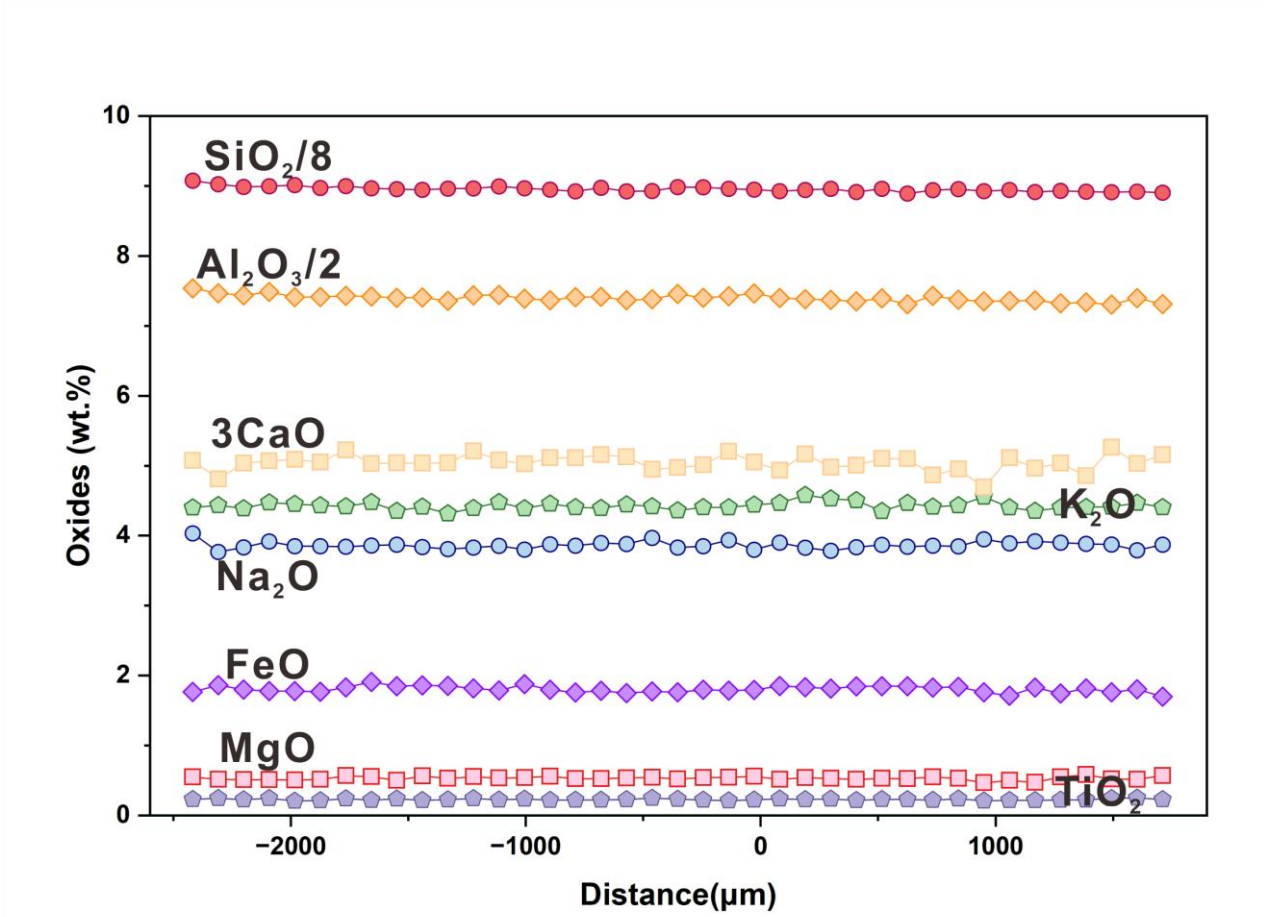

Figure S-2 Major element concentration profiles in wt.% from sample LSTAg2 (t = 569.4s at T = 1473K, P = 1 GPa) measured by EPMA.

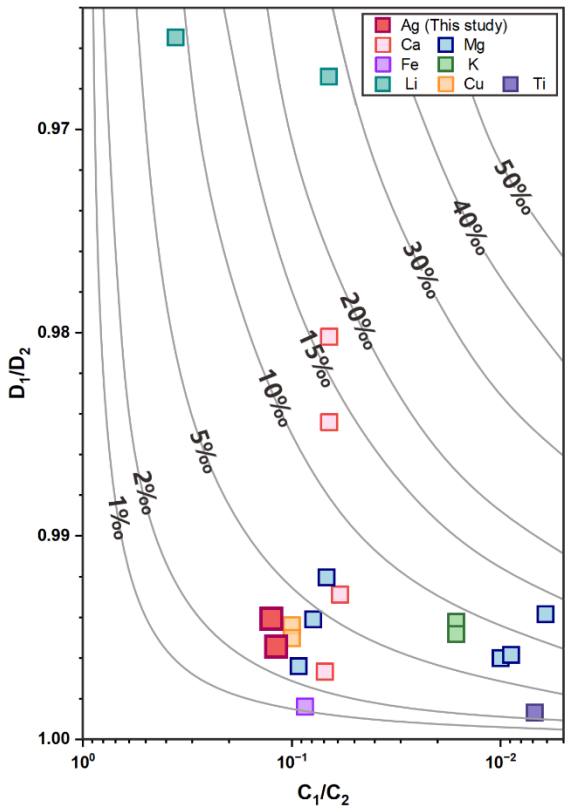

Figure S-3 Modelling of isotopic fractionation by diffusion, showing the degree of isotopic fractionation in relation to two key parameters (elemental concentration ratio, diffusion coefficient ratio). The elemental concentration ratio (C_1/C_2): the ratio of the concentration of the target element at both melts; and the diffusion coefficient ratio (D_1/D_2): the ratio of the isotope diffusion coefficients, usually expressed as $(m_2/m_1)^{\beta}$, provide an important theoretical framework for understanding isotope fractionation in natural samples.

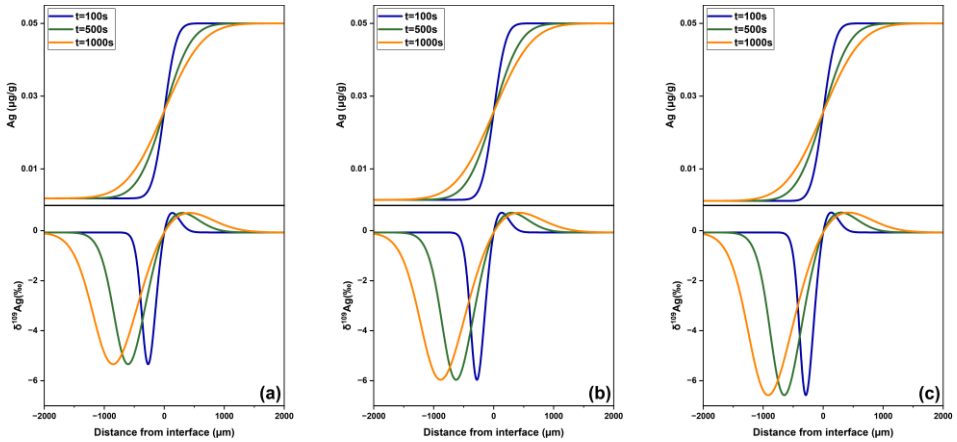

Figure S-4 Ag and δ^{109}Ag profiles when the magma upwells with fluid mass fractions of **(a)** 6 %, **(b)** 8 %, and **(c)** 10 %.

Supplementary Information References

Fang, Y., Wen, Q.-Y., Xiao, Z.-C., Yu, H.-M., Huang, F. (2024) High-precision measurement of Ag isotopes for silicate rocks by MC-ICP-MS. *Journal of Analytical Atomic Spectrometry* 39, 1750–1758. https://doi.org/10.1039/D3JA00424D

Hou, Z., Xiao, Y., Shen, J., Yu, C. (2020) In situ rutile U-Pb dating based on zircon calibration using LA-ICP-MS, geological applications in the Dabie orogen, China. *Journal of Asian Earth Sciences* 192, 104261. https://doi.org/10.1016/j.jseaes.2020.104261

Ni, H., Shi, H., Zhang, L., Li, W.-C., Guo, X., Liang, T. (2018) Cu diffusivity in granitic melts with application to the formation of porphyry Cu deposits. *Contributions to Mineralogy and Petrology* 173, 50. https://doi.org/10.1007/s00410-018-1475-0

Zhang, L., Guo, X., Li, W.-C., Ding, J., Bai, B., Ni, H. (2021) Rapid Ag diffusion in granitic melt: Implications for Ag mineralization and melt inclusion record. *Geochimica et Cosmochimica Acta* 310, 47–60. https://doi.org/10.1016/j.gca.2021.07.008

Zhang, P., Zhang, L., Wang, Z., Li, W.-C., Guo, X., Ni, H. (2018) Diffusion of molybdenum and tungsten in anhydrous and hydrous granitic melts. *American Mineralogist* 103, 1966–1974. https://doi.org/10.2138/am-2018-6569